KSCE Journal of Civil Engineering (2023) 27(6):2593-2602
DOI 10.1007/s12205-023-2029-1

pISSN 1226-7988, eISSN 1976-3808
www.springer.com/12205

Structural Engineering

Modulus of Subgrade Reaction for Circular Tunnels considering Bedrock and Ground Surface

Wusheng Zhao[a], **Peiyao Xie**[a,b], **Weizhong Chen**[a], **and Changkun Qin**[a]

[a]*State Key Laboratory of Geomechanics and Geotechnical Engineering, Institute of Rock and Soil Mechanics, Chinese Academy of Sciences, Wuhan 430071, China*
[b]*University of Chinese Academy of Sciences, Beijing 100049, China*

ARTICLE HISTORY

Received 31 October 2022
Revised 4 March 2023
Accepted 13 March 2023
Published Online 20 April 2023

KEYWORDS

Modulus of subgrade reaction
Tunnel
Bedrock
Ground surface
Deformation pattern

ABSTRACT

The modulus of subgrade reaction is a key parameter used in tunnel design. However, the existing analytical relations for determining the modulus mainly focus on deep tunnels in the homogeneous ground. Therefore, the complex variable method was used to develop analytical solutions for calculating the modulus of subgrade reaction for deep circular tunnels close to bedrock and shallow circular tunnels under uniform and oval deformation patterns. Subsequently, the analytical solutions were validated by comparing them with numerical solutions. At last, parametric studies were conducted to analyze the impacts of the bedrock and ground surface on the modulus of subgrade reaction. The results show that the modulus increases substantially near the bedrock and decreases slightly away from the bedrock, while the ground surface has the opposite effect. In addition, the effects of the bedrock and the ground surface on the radial modulus are more significant than that on the tangential modulus. Furthermore, the results confirm the effect of the tunnel deformation pattern on the modulus of subgrade reaction. The analytical solutions may be used for obtaining the approximate magnitude of the modulus of subgrade reaction in the structure design of shallow tunnels and deep tunnels close to bedrock.

1. Introduction

The Winkler model is extensively employed by engineers to solve soil-structure interaction problems (Dutta and Roy, 2002; Bouzid et al., 2013; Yu et al., 2014; Woo et al., 2018). The model idealizes the soil consisting of closely spaced, identical but mutually independent springs. The modulus of subgrade reaction (MSR) is one of the key parameters in the Winkler model, and it is defined as the ratio of the traction applied at the ground-tunnel interface divided by the corresponding deformation. Since the MSR affects the behavior of the tunnel lining significantly, it is crucial to obtain its magnitude accurately for the tunnel design (Kog et al., 2013).

The MSR is not a fundamental property of soil, and it is influenced by many factors, such as the buried depth of tunnel (Chen et al., 2016), the deformation pattern of ground (Ghiasi et al., 2012; Avci and Gurbuz, 2018), the ground properties, and the lining stiffness. Generally, the MSR can be determined by plate loading tests (Terzaghi, 1955; Dincer, 2011), empirical or analytical relations (Elachachi et al., 2004; Jamil and Ahmad, 2019), and numerical approaches (Matsubara and Hoshiya, 2000; Avci and Gurbuz, 2018). In comparison, numerical methods could consider more details, such as the plastic properties of soil (Ghiasi and Mozafari, 2018), the cracking of geomaterial (Zhang and Zhuang, 2018; 2019), and the failure of ground (Zhang et al., 2018, 2022). However, as the empirical or analytical relations could provide general solutions and are relatively simple, many empirical equations for determining the MSR have been proposed. Wood (1975) proposed an analytical solution to determine the MSR for a circular tunnel under an oval deformation pattern in elastic ground. Later, Luscher (1966), Okeagu and Abdel-Sayed (1984) developed similar relations for calculating the horizontal MSR for buried circular pipelines or tunnels. Matsubara and Hoshiya (2000) presented a solution for the longitudinal MSR of a buried pipeline for the seismic design. Based on the Wood's solution (1975), Zhang et al. (2014) used a Fourier series to describe the

CORRESPONDENCE Wusheng Zhao ✉ wszhao@whrsm.ac.cn State Key Laboratory of Geomechanics and Geotechnical Engineering, Institute of Rock and Soil Mechanics, Chinese Academy of Sciences, Wuhan 430071, China

radial deformation of tunnel, and presented a solution for the radial MSR. Guha et al. (2016) developed an analytical solution to determine the axial stiffness for pipelines and verified it by numerical analyses. Chen et al. (2016) assumed that the MSR increases linearly with the buried depth, and proposed a numerical approach for laterally loaded piles on elastic foundations. Basudhar et al. (2018) developed a new relation for the MSR by correlating the Winkler model and the maximum bending moments and deflection. In addition, many researchers (Kog et al., 2013; Prendergast and Gavin, 2016) discussed the suitability of different relations developed for determination of the MSR. As for the MSR in the tunnel design, the existing analytical studies mainly focus on deep tunnels in homogeneous ground, and the impact of the ground surface is neglected. However, the ground surface could affect the deformation pattern of shallow tunnels (Ghiasi and Koushki, 2020) and then the MSR. Besides, relatively little research concerning the effect of stratigraphic changes on the MSR has been undertaken. As a result, it is still difficult to calculate the appropriate magnitude of MSR for the structure design of shallow tunnels and tunnels close to the bedrock.

The main goal of this study was to establish analytical relations for the determination of the MSR for circular tunnels considering the effects of the bedrock and the ground surface. Two fundamental deformation patterns (uniform and oval) of circular tunnels (González and Sagaseta, 2001) were considered. The second objective was to investigate the influences of the bedrock and ground surface on the MSR. First, analytical solutions for the MSR for deep tunnels close to the bedrock and shallow tunnels near the ground surface were established using the complex variable method. Subsequently, the analytical solutions were validated by finite element (FE) analyses. At last, the effects of the ground surface and the bedrock on the MSR were analyzed by parametric studies. The analytical solutions could be used for obtaining the approximate magnitude of the MSR in the tunnel design.

2. Problem Description and Methodology

2.1 Problem Description

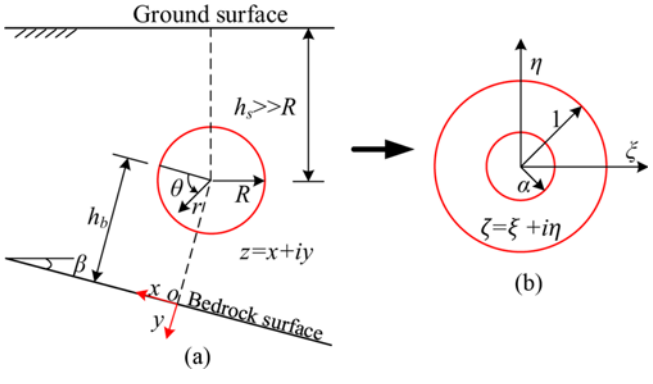

Fig. 1. A Deep Circular Tunnel Near the Bedrock: (a) The Original Region, (b) The Region of Conformal Transformation

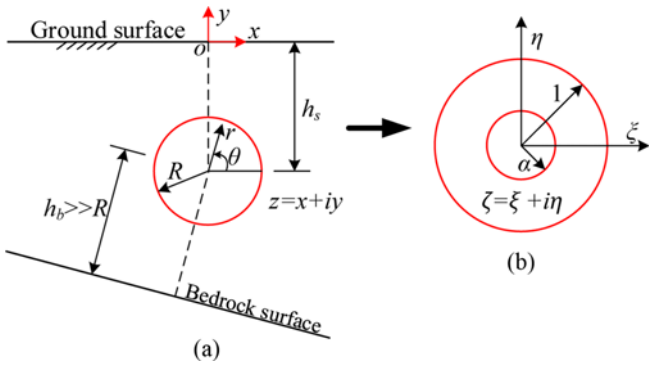

Fig. 2. A Shallow Circular Tunnel Near the Ground Surface: (a) The Original Region, (b) The Region of Conformal Transformation

As shown in Figs. 1 and 2, a circular tunnel is located in a homogeneous and elastic soil, and the ground surface is flat and free of stress. A plane-strain condition is assumed. β is the angle between the bedrock surface and the horizontal plane; R is the radius of tunnel; h_b is the distance from the tunnel center to the bedrock surface; h_s is the depth of the tunnel center below the ground surface. Two cases were considered in this study: deep tunnels close to bedrock (see Fig. 1) and shallow tunnels near the ground surface (see Fig. 2). For the former case, it is assumed that the depth of tunnel is much larger than the radius of tunnel, $h_s>>R$. Therefore, the influence of the ground surface can be neglected. Meanwhile, as the stiffness of the bedrock is much greater than that of the soil, the displacements at the bedrock surface owing to loads applied on the tunnel surface are nearly equal to zero. For the latter case, it is assumed that the tunnel is far from the bedrock, $h_b>>R$. The bedrock has little effect on the MSR for shallow tunnels. However, the ground surface can influence the stress and displacement in the soil around the tunnel and then the modulus of subgrade reaction.

2.2 Complex Variable Method

In this study, the analytical solution to the above problem was developed using the complex variable method. In the complex variable method (Timoshenko and Goodier, 1951), the normal stresses (σ_{xx}, σ_{yy}) and the shear stress (τ_{xy}) in the region z could be depicted by two analytic functions, $\phi(z)$ and $\psi(z)$ as follows:

$$\begin{aligned}\sigma_{xx}+\sigma_{yy}&=2\left[\phi'(z)+\overline{\phi'(z)}\right]\\ \sigma_{yy}-\sigma_{xx}+2i\tau_{xy}&=2\left[\bar{z}\phi''(z)+\psi'(z)\right],\end{aligned} \tag{1}$$

where $\overline{\ }$ refers to the conjugate operation; ' is the derivation operation; $i=\sqrt{-1}$; $z=x+iy$.

The displacements (u_x, u_y) in the region z expressed by the two analytic functions are

$$2G\left(u_x+iu_y\right)=\kappa\phi(z)-z\overline{\phi'(z)}-\overline{\psi(z)}, \tag{2}$$

where G is the shear modulus of ground; $k=3-4\nu$; ν is the Poisson's ratio of ground.

The boundary condition involving the surface traction is expressed as:

$$F = i\int_0^s \left(t_x + it_y\right)ds = \phi(z) + z\overline{\phi'(z)} + \overline{\psi(z)} + C\,, \tag{3}$$

where t_x and t_y are the tractions along the surface in the x and y directions, respectively; C is an constant.

The region z could be mapped conformally onto a ring in the region ζ shown in Figs. 1(b) and 2(b) (Verruijt, 1997), and the conformal transformation is

$$z = \omega(\zeta) = -ih\frac{1-\alpha^2}{1+\alpha^2}\frac{1+\zeta}{1-\zeta}\,, \tag{4}$$

where

$$\frac{R}{h} = \frac{2\alpha}{1+\alpha^2}\,, \tag{5}$$

where $h = h_b$ for deep tunnels close to bedrock and $h = h_s$ for shallow tunnels.

The outer boundary of the ring, $|\zeta| = 1$, corresponds to the bedrock surface in Fig. 1 (or the ground surface in Fig. 2). The inner boundary of the ring, $|\zeta| = \alpha$, corresponds to the tunnel surface, $z = Re^{i\theta} - hi$. Because the functions ϕ and ψ are analytic in both the region z and the region ζ, they could be expressed by Laurent series expansions:

$$\begin{aligned}\phi(z) &= \phi\left[\omega(\zeta)\right] = \sum_{k=0}^{\infty} a_k\zeta^k + \sum_{k=1}^{\infty} b_k\zeta^{-k}\\ \psi(z) &= \psi\left[\omega(\zeta)\right] = \sum_{k=0}^{\infty} c_k\zeta^k + \sum_{k=1}^{\infty} d_k\zeta^{-k}.\end{aligned} \tag{6}$$

2.3 Boundary Conditions

2.3.1 Boundary conditions for Deep Tunnels Close to Bedrock

Because the stiffness of the bedrock is assumed to be much greater than that of the soil, the displacements at the bedrock surface owing to loads applied on the tunnel surface are nearly equal to zero. From Eqs. (2) and (4), the boundary condition in the region ζ can be expressed as:

$$\zeta = \sigma:\ \kappa\phi(\zeta) - \frac{\omega(\zeta)}{\overline{\omega'(\zeta)}}\overline{\phi'(\zeta)} - \overline{\psi(\zeta)} = 0\,, \tag{7}$$

where $\sigma = e^{i\theta}$ represents a circle with a radius of 1.0 in the region ζ.

Substituting Eqs. (4) – (6) into Eq. (7), the following equations can be obtained:

$$\begin{aligned}c_0 &= \kappa\overline{a_0} - \frac{1}{2}a_1 - \frac{1}{2}b_1\\ \overline{c_k} &= \kappa\overline{b_k} + \frac{1}{2}(k-1)a_{k-1} - \frac{1}{2}(k+1)a_{k+1}, (k\ge 1)\\ \overline{d_k} &= \kappa\overline{a_k} + \frac{1}{2}(k-1)b_{k-1} - \frac{1}{2}(k+1)b_{k+1},\ (k\ge 1).\end{aligned} \tag{8}$$

If a prescribed traction, $t(z) = t[\omega(\zeta)] = T(\zeta)$, is applied along the tunnel surface, from Eq. (3), the boundary condition in the region ζ can be written as:

$$\zeta = \alpha\sigma:\ \phi(\zeta) + \frac{\omega(\zeta)}{\omega'(\zeta)}\overline{\phi'(\zeta)} + \overline{\psi(\zeta)} = T(\zeta)\,. \tag{9}$$

Similarly, the function, $T(\zeta)$, can be expressed as a Fourier series,

$$T(\zeta) = \frac{1}{1-\alpha\sigma}\sum_{k=-\infty}^{k=\infty} A_k\sigma^k\,. \tag{10}$$

Substituting Eqs. (4), (6), (8), and (10) into Eq. (9) gives

$$\begin{aligned}&\left(\alpha^2-1\right)(k+1)\overline{a_{k+1}} - \left(\alpha^{-2k} + \kappa\alpha^2\right)b_{k+1} =\\ &\quad\left(\alpha^2-1\right)k\overline{a_k} - \left(\alpha^{-2k}+\kappa\right)b_k + \alpha^{-k}A_{-k}\\ &\left(\alpha^{2k+2}+\kappa\right)\overline{a_{k+1}} - \left(1-\alpha^2\right)(k+1)b_{k+1} =\\ &\quad\left(\alpha^{2k+2}+\kappa\alpha^2\right)\overline{a_k} - \left(1-\alpha^2\right)(k)b_k + \overline{A_{k+1}}\alpha^{k+1},\end{aligned} \tag{11}$$

and

$$\begin{aligned}\left(\alpha^2-1\right)\overline{a_1} - \left(1+\kappa\alpha^2\right)b_1 &= A_0 - (1+\kappa)a_0\\ \left(\alpha^2+\kappa\right)\overline{a_1} - \left(1-\alpha^2\right)b_1 &= \overline{A_1}\alpha + (1+\kappa)\alpha^2\overline{a_0}\,.\end{aligned} \tag{12}$$

2.3.2 Boundary Conditions for Shallow Tunnels Near Ground Surface

The ground surface is flat and free of stress. From Eq. (3), the boundary condition in the region ζ can be written as:

$$\zeta = \sigma:\ \phi(\zeta) + \frac{\omega(\zeta)}{\overline{\omega'(\zeta)}}\overline{\phi'(\zeta)} + \overline{\psi(\zeta)} = 0\,. \tag{13}$$

Substituting Eqs. (4) – (6) into Eq. (13), the following equations can be obtained:

$$\begin{aligned}c_0 &= -\overline{a_0} - \frac{1}{2}a_1 - \frac{1}{2}b_1\\ c_k &= -\overline{b_k} + \frac{1}{2}(k-1)a_{k-1} - \frac{1}{2}(k+1)a_{k+1},\quad (k\ge 1)\\ d_k &= -\overline{a_k} + \frac{1}{2}(k-1)b_{k-1} - \frac{1}{2}(k+1)b_{k+1},\quad (k\ge 1).\end{aligned} \tag{14}$$

If a displacement boundary, $u(z) = u[\omega(\zeta)] = D(\zeta)$, is prescribed along the tunnel surface, and the function, $D(\zeta)$, can be expressed as a Fourier series,

$$D(\zeta) = \frac{1}{1-\alpha\sigma}\sum_{k=-\infty}^{k=\infty} A_k\sigma^k\,. \tag{15}$$

Verruijt (1997) has presented the coefficients as follows:

$$\begin{aligned}&\left(1-\alpha^2\right)(k+1)\overline{a_{k+1}} - \left(a^2 + \kappa\alpha^{-2k}\right)b_{k+1} =\\ &\quad\left(1-\alpha^2\right)k\overline{a_k} - \left(1+\kappa\alpha^{-2k}\right)b_k + A_{-k}\alpha^{-k}\\ &\left(1+\kappa\alpha^{2k+2}\right)\overline{a_{k+1}} + \left(1-\alpha^2\right)(k+1)b_{k+1} =\\ &\quad\alpha^2\left(1+\kappa\alpha^{2k}\right)\overline{a_k} - \left(1-\alpha^2\right)kb_k + \overline{A_{k+1}}\alpha^{k+1},\end{aligned} \tag{16}$$

and

$$\begin{aligned}&\left(1-\alpha^2\right)\overline{a_1}-\left(\alpha^2+\kappa\right)b_1=A_0-\left(1+\kappa\right)a_0\\&\left(1+\kappa\alpha^2\right)\overline{a_1}+\left(1-\alpha^2\right)b_1=\overline{A_1}\alpha+\alpha^2\left(1+\kappa\right)\overline{a_0}\,.\end{aligned}\tag{17}$$

2.4 Procedure for Determining MSR

The MSR can be determined by the following steps:

1. The coefficients A_k are determined by the boundary conditions applied on the tunnel surface. The formulations of the coefficients for the uniform and oval deformation patterns of circular tunnels will be established in the following section.
2. The series expansions of the functions, ϕ and ψ, should converge at infinity, by which the coefficient a_0 can be determined. The process is as follows: assuming $a_0 = 0$, the coefficient for deep tunnels close to the bedrock, $b_k(k\to\infty) = s_0$, could be calculated by Eqs. (11) and (12). The coefficient for shallow tunnels, $b_k(k\to\infty) = s_0$, could be calculated by Eqs. (16) and (17). Similarly, assuming $a_0 = 1+i$, and calculating the coefficient, $b_k(k\to\infty) = s_1$. The coefficient a_0 can be determined by $a_0 = s_0/(s_0-s_1)$.
3. For deep tunnels close to the bedrock, the coefficients, a_k and b_k, could be determined from the recurrent Eqs. (11) and (12). Subsequently, the coefficients, c_k and d_k, could be calculated from Eq. (8). For shallow tunnels, the coefficients, a_k and b_k, could be determined from Eqs. (16) and (17). Subsequently, the coefficients, c_k and d_k, could be obtained from Eq. (14).
4. After all the coefficients (a_k, b_k, c_k, and d_k) are determined, the functions ϕ and ψ can be obtained by Eq. (6). Subsequently, the stresses and displacements in the soil can be calculated from Eqs. (1) and (2), respectively. At last, the MSR can be determined by dividing the stress by the corresponding displacement.

For a tunnel in an infinite, elastic ground, from the theory of elasticity, both the radial and tangential moduli of subgrade reaction are equal to $2G/R$ (Zhang et al., 2014). In order to highlight the influence of the bedrock or the ground surface, the MSR is normalized by the magnitude, $2G/R$, in this study.

3. Modulus of Subgrade Reaction for Different Deformation Patterns of Tunnel

As long as the coefficients of Fourier series, A_k, in Eqs. (10) or (15) are determined, the MSR can be calculated by the procedure presented in section 2.4. Therefore, the coefficients of Fourier series, A_k, for different deformation patterns of tunnel are presented in this section.

3.1 Solution for Deep Tunnels Close to Bedrock under a Uniform Deformation Pattern

3.1.1 Radial Modulus of Subgrade Reaction

If a uniform radial traction, $t(z) = t_0$, is applied on the tunnel surface, the function, $T(\zeta)$, in the region ζ is:

$$T(\zeta)=\frac{2ih_bt_0\alpha}{\left(1+\alpha^2\right)\left(1-\alpha\sigma\right)}\left[\alpha-\sigma+i\left(1-\zeta\right)\right].\tag{18}$$

Substituting Eq. (18) into Eq. (10) gives

$$\begin{aligned}&A_0=\frac{2ih_b\alpha t_0}{1+\alpha^2}\left(\alpha+i\right),\quad A_1=-\frac{2ih_b\alpha t_0}{1+\alpha^2}\left(1+i\alpha\right)\\&A_k=0,\quad\left(k\neq0,k\neq1\right).\end{aligned}\tag{19}$$

3.1.2 Tangential Modulus of Subgrade Reaction

If a uniform tangential traction, $t(z) = s_0$, is applied on the tunnel surface, the function, $T(\zeta)$, in the region ζ can be written as:

$$T(\zeta)=\frac{-2h_b\alpha t_0}{\left(1+\alpha^2\right)\left(1-\alpha\sigma\right)}\left[\alpha-\sigma+i\left(1-\zeta\right)\right].\tag{20}$$

Substituting Eq. (20) into Eq. (10) gives

$$\begin{aligned}&A_0=\frac{-2h_b\alpha t_0}{1+\alpha^2}\left(\alpha+i\right),\quad A_1=\frac{2h_b\alpha t_0}{1+\alpha^2}\left(1+\alpha i\right)\\&A_k=0,\quad\left(k\neq0,k\neq1\right).\end{aligned}\tag{21}$$

3.1.3 Validation of the Solution for Uniform Deformation Pattern

The analytical solutions in Eqs. (19) and (21) were validated by comparing them with the finite element (FE) solutions. A circular tunnel with a radius of 1.0 m is assumed to be located in a homogeneous and elastic soil. The depth of tunnel is large enough. Therefore, the effect of the ground surface can be neglected. The tunnel is close to the bedrock, and the distance from the tunnel center to the bedrock surface is 2.0 m. The FE model and the soil property are shown in Fig. 3. The top boundary is assumed to be the bedrock surface, and a plane-strain condition is assumed. The displacements in both the horizontal and vertical directions are fixed along the top boundary, and a uniform radial or tangential traction is applied on the tunnel surface to calculate the radial or tangential modulus of subgrade reaction. The FE software ABAQUS was used to conduct the numerical analysis. As shown in Fig. 4, both the radial and tangential moduli of

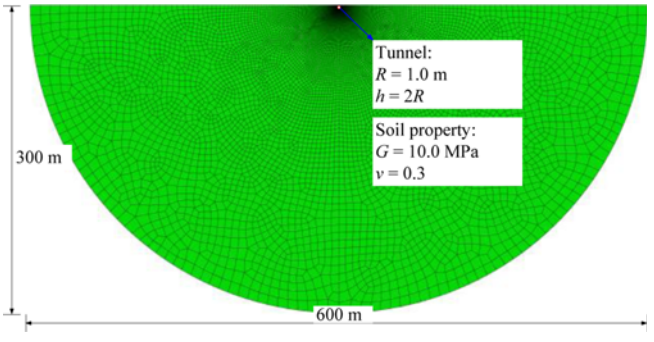

Fig. 3. Finite Element (FE) Model

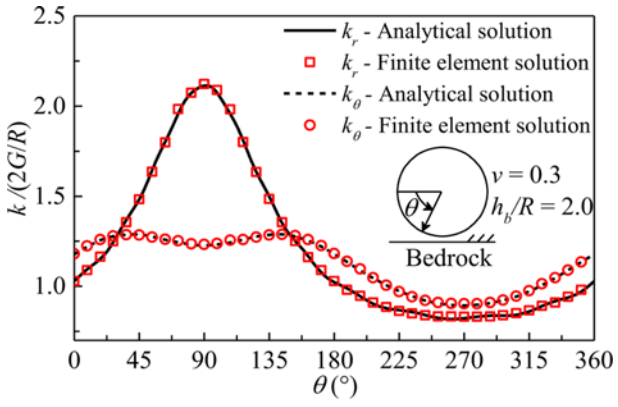

Fig. 4. Moduli of Subgrade Reaction for Deep Tunnels Close to Bedrock Calculated by Numerical and Analytical Approaches under a Uniform Traction

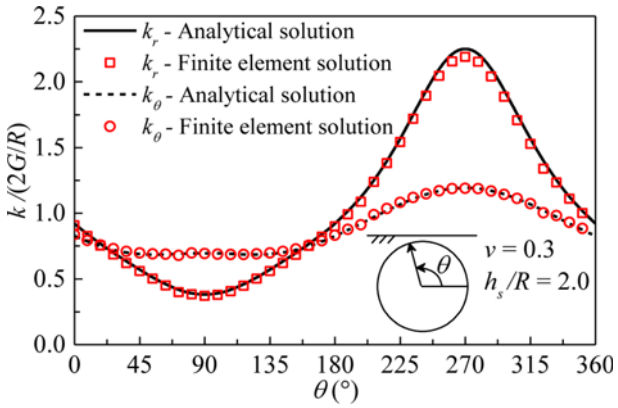

Fig. 5. Moduli of Subgrade Reaction for Shallow Tunnels Calculated By Numerical and Analytical Approaches under a Uniform Displacement

subgrade reaction calculated by the analytical method agree with that by the FE approach, which verifies the accuracy of the analytical solution.

3.2 Solution for Shallow Tunnels under a Uniform Deformation Pattern

3.2.1 Radial Modulus of Subgrade Reaction

If a uniform radial displacement, $u_r = u_0$, is prescribed on the tunnel surface, the coefficients of the Fourier series in Eq. (15) are

$$A_0 = 2iGu_0\alpha, \quad A_1 = -2iGu_0$$
$$A_k = 0, \ (k \neq 0, k \neq 1)\cdot \tag{22}$$

3.2.2 Tangential Modulus of Subgrade Reaction

If a uniform tangential displacement, $u_\theta = v_0$, is prescribed on the tunnel surface, the coefficients of Fourier series in Eq. (15) are

$$A_0 = -2Gv_0\alpha, \ A_1 = 2Gv_0$$
$$A_k = 0, \ (k \neq 0, k \neq 1)\cdot \tag{23}$$

3.2.3 Validation of the Solution for Uniform Deformation Pattern

The analytical solutions in Eqs. (22) and (23) were validated by comparing them with the FE solutions. A circular and shallow tunnel is considered here. The tunnel with a radius of 1.0 m is located in an elastic half space, and the depth of tunnel is 2.0 m. The ground surface is flat and free of tractions. The FE model shown in Fig. 3 is used to verify the analytical solution for shallow tunnels under a uniform displacement along the tunnel surface ($u_r = u_0$ or $u_\theta = v_0$). The top boundary is assumed to be the ground surface, and the displacements in both x and y directions at outer boundary are fixed. It can be found from Fig. 5 that both the radial and tangential moduli of subgrade reaction calculated by the analytical method are consistent with that by the FE approach.

3.3 Solution for Shallow Tunnels under an Oval Deformation Pattern

The expressions of the coefficients of Fourier series, A_k, in Eq. (15) are derived for the oval deformation pattern of tunnel in this section. The detailed process is presented in Appendix.

3.3.1 Radial Modulus of Subgrade Reaction

If an oval radial displacement, $u_r = u_0\sin(2\theta)$, is applied on the tunnel surface, the displacement boundary condition in the region ζ is

$$D(\zeta) = \frac{Gu_0(1-\alpha^2)}{\alpha}\frac{(\alpha+\alpha^3)\sigma^{-2} - 4\alpha^2\sigma^{-1} + 4\alpha^2\sigma^{1} - (\alpha+\alpha^3)\sigma^{2}}{(1-\alpha\sigma)^2(1-\alpha\sigma^{-1})^2}\frac{(\alpha-\sigma)}{1-\alpha\sigma}. \tag{24}$$

Substituting Eq. (24) into Eq. (15) and using series expansion gives (see Appendix)

$$A_0 = \frac{2Gu_0\alpha}{(1-\alpha^2)}\left[\alpha^4 - \alpha^2 + 2 + \frac{\alpha^4-1}{1-\alpha^2}\right]$$
$$A_1 = \frac{Gu_0}{\alpha(1-\alpha^2)}\left[2\alpha^7 - 2\alpha^5 - 4\alpha^3 + \frac{2}{1-\alpha^2}(\alpha^7 - 4\alpha^5 + 3\alpha^3)\right]$$
$$A_2 = \frac{Gu_0}{\alpha(1-\alpha^2)}\left[3\alpha^8 - 7\alpha^6 + 3\alpha^4 - 3\alpha^2 + \frac{2}{1-\alpha^2}(\alpha^8 - 4\alpha^6 + 3\alpha^4)\right]$$
$$A_3 = \frac{Gu_0}{\alpha(1-\alpha^2)}\left[4\alpha^9 - 11\alpha^7 + 9\alpha^5 + \alpha^3 + \alpha + \frac{2}{1-\alpha^2}(\alpha^9 - 4\alpha^7 + 7\alpha^5 - 4\alpha^3)\right]$$
$$A_k = \frac{Gu_0\alpha^{k-3}}{(1-\alpha^2)}\left[(\alpha^8 + \alpha^6 - 9\alpha^4 + 11\alpha^2 - 4) + \frac{2+k(1-\alpha^2)}{1-\alpha^2}(\alpha^8 - 4\alpha^6 + 6\alpha^4 - 4\alpha^2 + 1)\right], \quad (k \geq 4)$$
$$A_{-k} = \frac{Gu_0\alpha^{k-1}}{(1-\alpha^2)}\left[\alpha^6 - 3\alpha^4 + 3\alpha^2 - 1\right], \ (k \geq 1)\cdot \tag{25}$$

Similarly, if an oval radial displacement, $u_r = u_0\cos(2\theta)$, is applied on the tunnel surface, the displacement boundary condition in the region ζ is

$$D(\zeta) = 2Gu_0\frac{(\alpha-\sigma)}{1-\alpha\sigma}\left[\frac{(1-\alpha^2)^2(\sigma^{-2} - 2 + \sigma^2)}{2(1-\alpha\sigma)^2(1-\alpha\sigma^{-1})^2} + 1\right]. \tag{26}$$

Substituting Eq. (26) into Eq. (15) and using the derivation procession similar to that in Appendix gives

$$\begin{aligned} &A_0 = -2Gu_0 i\alpha,\ A_1 = 2Gu_0 i\left(2\alpha^2 - \alpha^4\right) \\ &A_{-k} = Gu_0 i\left(\alpha^2 - 1\right)^2 \alpha^{k-1},\ \ (k \ge 1) \\ &A_k = Gu_0 i\left(\alpha^2 - 1\right)^2 \alpha^{k-3}\left[\left(1-\alpha^2\right)(k+1) - 3\right],\ (k \ge 2). \end{aligned} \tag{27}$$

3.3.2 Tangential Modulus of Subgrade Reaction

When an oval tangential displacement, $u_\theta = v_0\cos(2\theta)$, is applied on the tunnel surface, the displacement boundary condition in the region ζ can be written as:

$$D(\zeta) = -2Gv_0 i\frac{(\alpha-\sigma)}{1-\alpha\sigma}\left[\frac{\left(1-\alpha^2\right)^2\left(\sigma^{-2}-2+\sigma^2\right)}{2(1-\alpha\sigma)^2\left(1-\alpha\sigma^{-1}\right)^2}+1\right] \tag{28}$$

Substituting Eq. (28) into Eq. (15) and using the derivation procession similar to that in Appendix gives

$$\begin{aligned} &A_0 = 2Gv_0\alpha,\ A_1 = 2Gv_0\left(\alpha^4 - 2\alpha^2\right) \\ &A_k = Gv_0\left(\alpha^2-1\right)^2\alpha^{k-3}\left[3+\left(\alpha^2-1\right)(k+1)\right],\ (k \ge 2) \\ &A_{-k} = -Gv_0\left(\alpha^2-1\right)^2\alpha^{k-1},\ (k \ge 1) \end{aligned} \tag{29}$$

Similarly, if an oval tangential displacement, $u_\theta = v_0\sin(2\theta)$, is applied on the tunnel surface, the displacement boundary condition in the region ζ can be written as:

$$D(\zeta) = \frac{Gv_0 i\left(1-\alpha^2\right)}{\alpha}\frac{\left(\alpha+\alpha^3\right)\sigma^{-2} - 4\alpha^2\sigma^{-1} + 4\alpha^2\sigma^1 - \left(\alpha+\alpha^3\right)\sigma^2}{(1-\alpha\sigma)^2\left(1-\alpha\sigma^{-1}\right)^2}\frac{(\alpha-\sigma)}{1-\alpha\sigma}. \tag{30}$$

Substituting Eq. (30) into Eq. (15) and using the derivation procession similar to that in Appendix gives

$$\begin{aligned} &A_0 = \frac{2Gv_0 i\alpha}{\left(1-\alpha^2\right)}\left[\alpha^4 - \alpha^2 + 2 + \frac{\alpha^4-1}{1-\alpha^2}\right] \\ &A_1 = \frac{Gv_0 i}{\alpha\left(1-\alpha^2\right)}\left[2\alpha^7 - 2\alpha^5 - 4\alpha^3 + \frac{2}{1-\alpha^2}\left(\alpha^7 - 4\alpha^5 + 3\alpha^3\right)\right] \\ &A_2 = \frac{Gv_0 i}{\alpha\left(1-\alpha^2\right)}\left[3\alpha^8 - 7\alpha^6 + 3\alpha^4 - 3\alpha^2 + \frac{2}{1-\alpha^2}\left(\alpha^8 - 4\alpha^6 + 3\alpha^4\right)\right] \\ &A_3 = \frac{Gv_0 i}{\alpha\left(1-\alpha^2\right)}\left[4\alpha^9 - 11\alpha^7 + 9\alpha^5 + \alpha^3 + \alpha + \frac{2}{1-\alpha^2}\left(\alpha^9 - 4\alpha^7 + 7\alpha^5 - 4\alpha^3\right)\right] \\ &A_k = \frac{Gv_0 i\alpha^{k-3}}{\left(1-\alpha^2\right)}\left[\left(\alpha^8 + \alpha^6 - 9\alpha^4 + 11\alpha^2 - 4\right) + \frac{2+k\left(1-\alpha^2\right)}{1-\alpha^2}\left(\alpha^8 - 4\alpha^6 + 6\alpha^4 - 4\alpha^2 + 1\right)\right], \\ &\qquad (k \ge 4) \\ &A_{-k} = \frac{Gv_0 i\alpha^{k-1}}{\left(1-\alpha^2\right)}\left[\alpha^6 - 3\alpha^4 + 3\alpha^2 - 1\right],\ (k \ge 1). \end{aligned} \tag{31}$$

3.3.3 Linear Superposition of the Tunnel Deformation

Because the system is linear, the coefficients A_k in Eq. (15) for other deformation patterns can be determined by the linear superposition. For example, a circular tunnel is excited by a horizontal ground motion associated with vertically propagating shear-waves, the oval deformation along the tunnel surface can be written as:

$$\begin{aligned} u_r &= u_0\sin(2\theta) \\ u_\theta &= v_0\left[\cos(2\theta) - 1\right]. \end{aligned} \tag{32}$$

If $u_0 = v_0$, the deformation pattern corresponds to the free-field deformation. The coefficients A_k in Eq. (15) for this deformation pattern can be determined by adding Eq. (25) plus Eq. (29) minus Eq. (23).

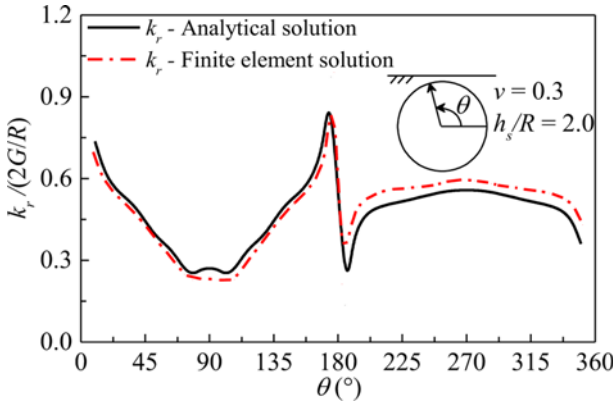

Fig. 6. Radial Moduli of Subgrade Reaction for Shallow Tunnels Calculated by Numerical and Analytical Approaches under an Oval Deformation Pattern

3.3.4 Validation of the Solution for Oval Deformation Pattern

The analytical solution for the oval deformation pattern was validated by comparing it with the FE solution. A circular and shallow tunnel is considered. The tunnel with a radius of 1.0 m is located in an elastic half space, and the depth of tunnel is 2.0 m. The ground surface is flat and free of traction. The FE model shown in Fig. 3 is used to validate the analytical solution for the free-field deformation pattern in Eq. (32), $u_0 = v_0$. The top boundary (ground surface) is free from stress, and the displacements at the outer boundary are constrained. The calculated radial MSRs for this deformation pattern are shown in Fig. 6. It can be seen that the moduli calculated by the analytical solution agree with the FE solution, which indicates the analytical solution and the superposition method are correct.

4. Effects of Bedrock and Ground Surface on Modulus of Subgrade Reaction

4.1 Effect of Bedrock on Modulus of Subgrade Reaction

A parametric study was carried out to analyze the impact of the bedrock on the moduli of subgrade reaction. The FE model shown in Fig. 3 is considered, and the top boundary is assumed to be the bedrock surface. A uniform radial or tangential traction is applied on the tunnel surface. As shown in Fig. 7, the distribution of the MSR along the tunnel surface is non-uniform owing to the

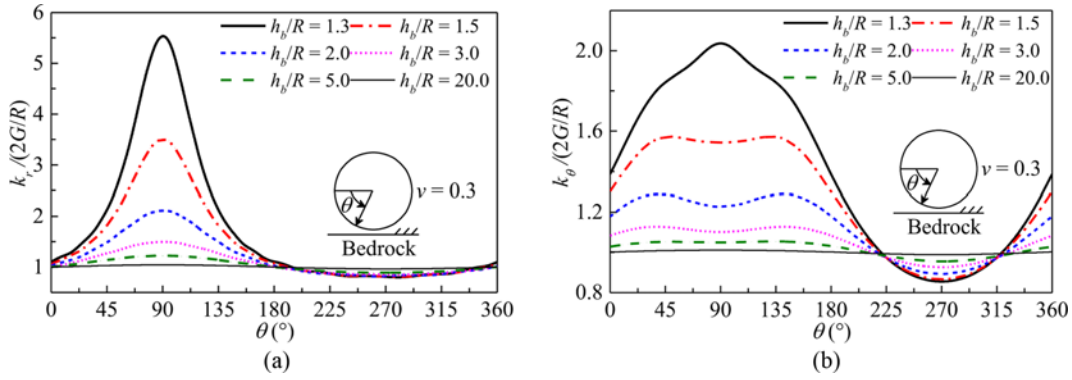

Fig. 7. Modulus of Subgrade Reaction versus the Distance from Tunnel Center to Bedrock Surface under a Uniform Traction: (a) Radial Modulus, (b) Tangential Modulus

bedrock. The radial moduli of subgrade reaction below the tunnel center are larger than 1.0, while the moduli above the tunnel center are nearly equal to 1.0. The maximum radial modulus occurs at the location closest to the bedrock surface, $\theta = 90°$. The tangential moduli at the locations, $\theta = 225° - 315°$, are slightly smaller than 1.0, and the moduli at other locations are larger than 1.0. The location where the maximum tangential modulus occurs varies for different cases. In comparison, the effect of the bedrock on the radial MSR is more remarkable than that on the tangential MSR. As the distance (h_b) increases, both the radial and tangential moduli tend to be 1.0 that corresponds to the value for deep tunnels in the homogeneous ground. It can be seen from Fig. 8 that for a given distance ($h_b/R = 2.0$), as the Poisson's ratio of the soil increases, the maximum radial MSR increases, while the maximum tangential MSR decreases.

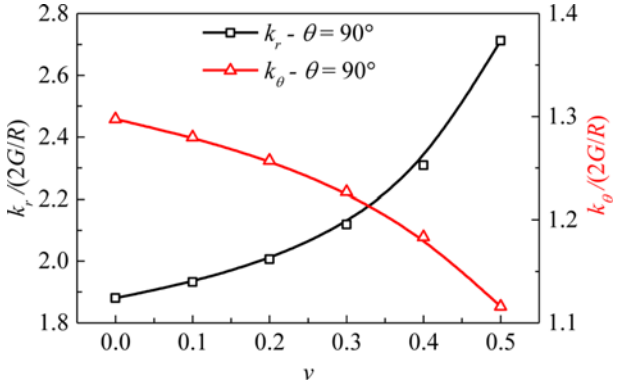

Fig. 8. Variations of the Maximum Radial and Tangential Moduli of Subgrade Reaction for Deep Tunnels ($h_b/R = 2.0$) with the Poisson's Ratio of Soil

4.2 Effect of Ground Surface on Modulus of Subgrade Reaction

Parametric studies were carried out to examine the effects of the ground surface on the modulus of subgrade reaction under the uniform and oval deformation patterns. The FE model shown in Fig. 3 is considered, and the top boundary is assumed to be the ground surface. A uniform or oval deformation is applied on the tunnel surface. As shown in Fig. 9, despite the uniform deformation pattern, the MSR along the tunnel surface is not uniform owing to the ground surface. The radial MSR below the tunnel center is larger than 1.0, while the radial MSR above the tunnel center is smaller than 1.0. The tangential MSR below the knee of tunnel ($\theta = 225° - 315°$) is slightly larger than 1.0, and it is smaller than 1.0 at other locations. The minimum MSR occurs at the crown of tunnel, while the maximum modulus occurs at the invent of tunnel. As the depth of tunnel increases, both the radial and

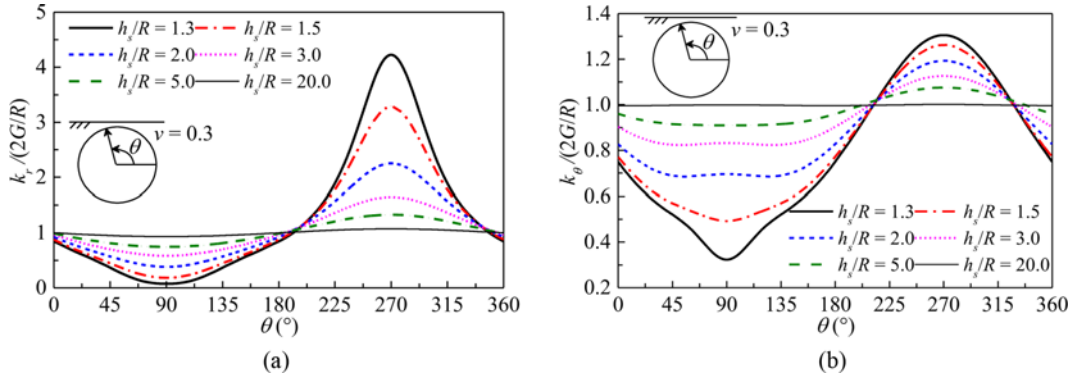

Fig. 9. Variations of Modulus of Subgrade Reaction with the Depth of Tunnel under a Uniform Deformation: (a) Radial Modulus under $u_r = u_0$, (b) Tangential Modulus under $u_\theta = v_0$

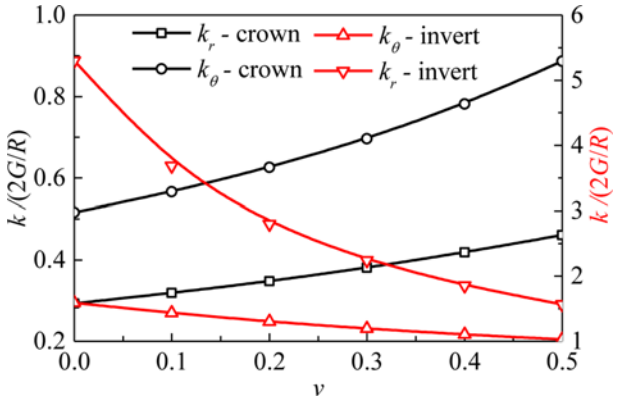

Fig. 10. Radial and Tangential Moduli of Subgrade Reaction at the Crown and Invert of Tunnel versus the Poisson's Ratio of Soil under a Uniform Deformation Pattern

tangential MSRs tend to be 1.0. In comparison, the effect of the ground surface on the radial MSR is more remarkable than that on the tangential MSR. It can be seen from Fig. 10 that for a given depth of tunnel (h_s/R = 2.0), as the Poisson's ratio of the soil increases, both the radial and tangential moduli of subgrade reaction at the crown of tunnel increase, while the moduli at the invert of tunnel decrease. The result indicates that the MSR along the tunnel surface becomes more uniform with increment of the Poisson's ratio.

Figure 11 presents the radial and tangential moduli of subgrade reaction for two oval deformation patterns. As shown, the radial or tangential MSR above the tunnel center is smaller than that below the tunnel center owing to the ground surface. However, the distribution of the radial MSR along the tunnel surface is different from that of the tangential MSR. In comparison with the uniform deformation pattern (see Fig. 9), significant differences can be found with respect to both the magnitude and the MSR distribution along the tunnel surface. The MSR distribution along the tunnel surface is more non-uniform for oval deformation pattern, and the MSR changes suddenly at several locations such as the crown and the invert of tunnel for $u_r = u_0\sin(2\theta)$, and the shoulder and the knee of tunnel for $u_\theta = v_0\cos(2\theta)$. When the depth of tunnel is large enough, the MSR for the oval deformation pattern is still greater than that for the uniform deformation pattern, which confirms that the deformation pattern could significantly affect the MSR.

5. Conclusions

Analytical solutions were developed to estimate the MSR for deep circular tunnels close to the bedrock and shallow circular tunnels near the ground surface under two fundamental deformation patterns (uniform and oval). The solutions were validated by FE analyses, and the effects of the bedrock and the ground surface on the MSR were investigated as well. The main conclusions are as follows:

1. For deep tunnels close to the bedrock, the bedrock has a significant effect on the MSR, and the effect on the radial MSR is more significant than that on the tangential MSR. Compared with the case without bedrock, the MSR becomes much larger on the side near the bedrock and slightly smaller on the other side under the uniform deformation pattern. The smaller the distance from the tunnel center to the bedrock, the more pronounced this effect is. As the Poisson's ratio of the soil increases, the effect of the bedrock on the radial MSR becomes more significant, while the effect of the bedrock on the tangential MSR becomes less notable.
2. For shallow tunnels near the ground surface, the ground surface could greatly influence the MSR. Compared with deep tunnels in the homogeneous soil, both the radial and tangential moduli of subgrade reaction at locations above the tunnel center decrease, while they increase at locations below the tunnel center. The smaller the depth of tunnel and the smaller the Poisson's ratio of soil, the more significant this effect is. In comparison with the MSR under the uniform deformation pattern, the MSR distribution along the tunnel surface under the oval deformation pattern is more non-uniform. Moreover, the distribution of the radial MSR along the tunnel surface is different from that of the tangential modulus.

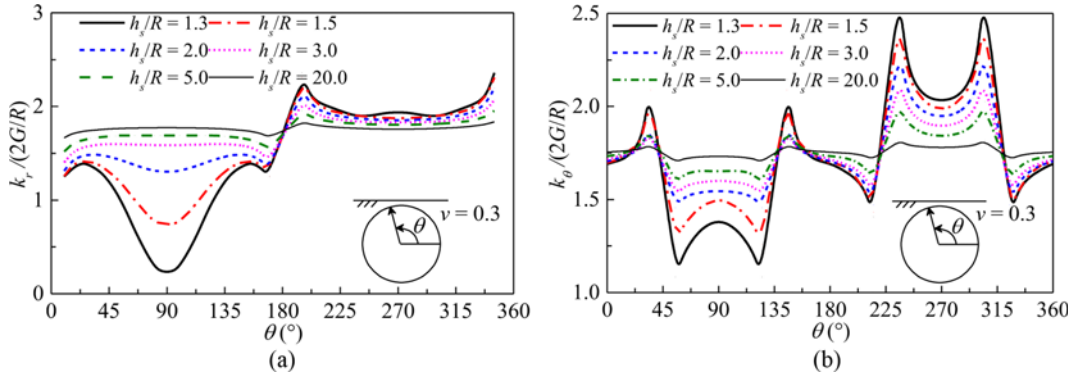

Fig. 11. Variations of Modulus of Subgrade Reaction with the Depth of Tunnel under an Oval Deformation: (a) Radial MSR under $u_r = u_0\sin(2\theta)$, (b) Tangential MSR under $u_\theta = v_0\cos(2\theta)$

3. The results confirm the significant effect of the tunnel deformation pattern on the MSR. Consequently, the MSR should be determined carefully based on the tunnel deformation in practice.

The analytical solutions were derived using the theory of elasticity in this study, which cannot describe the inelastic properties of soil. Besides, the tunnel lining was not considered in the derivation. In spite of the limitations, the analytical solutions may be used to obtain an approximate magnitude of the MSR for the preliminary design of circular tunnels. In addition, the analytical solutions can offer benchmarks to verify numerical results.

Acknowledgments

This work was supported by the National Natural Science Foundation of China (Grant numbers 52079134, 51991393).

ORCID

Wusheng Zhao http://orcid.org/0000-0001-5204-0205
Peiyao Xie http://orcid.org/0009-0004-8904-8357
Weizhong Chen http://orcid.org/0000-0002-6509-8411
Changkun Qin http://orcid.org/0000-0002-6449-1940

References

Avci B, Gurbuz A (2018) Modulus of subgrade reaction that varies with magnitude of displacement of cohesionless soil. *Arabian Journal of Geosciences* 11:351, DOI: 10.1007/s12517-018-3713-1

Basudhar PK, Yadav SK, Basudhar A (2018) Treatise on winkler modulus of subgrade reaction and its estimation for improved soil–structure interaction analysis. *Geotechnical and Geological Engineering* 36: 3091-3109, DOI: 10.1007/s10706-018-0523-x

Bouzid DA, Bhattacharya S, Dash SR (2013) Winkler Springs (p-y curves) for pile design from stress-strain of soils: FE assessment of scaling coefficients using the Mobilized Strength Design concept. *Geomechanics and Engineering* 5(5):379-399, DOI: 10.12989/gae.2013.5.5.379

Chen JL, Feng YQ, Shu WY (2016) An improved solution for beam on elastic foundation using quintic displacement functions. *KSCE Journal of Civil Engineering* 20(2):792-802, DOI: 10.1007/s12205-015-0424-y

Dincer I (2011) Models to predict the deformation modulus and the coefficient of subgrade reaction for earth filling structures. *Advances in Engineering Software* 42(4):160-171, DOI: 10.1016/j.advengsoft.2011.02.001

Dutta SC, Roy R (2002) A critical review on idealization and modeling for interaction among soil–foundation–structure system. *Computers and Structures* 80:1579-1594, DOI: 10.1016/S0045-7949(02)00115-3

Elachachi SM, Breysse D, Houy L (2004) Longitudinal variability of soils and structural response of sewer networks. *Computers and Geotechnics* 31(8):625-641, DOI: 10.1016/j.compgeo.2004.10.003

Ghiasi V, Ghiasi S, Prasad A (2012) Evaluation of tunnels under squeezing rock condition. *Journal of Engineering, Design and Technology* 10(2):168-179, DOI: 10.1108/17260531211241167

Ghiasi V, Koushki M (2020) Numerical and artificial neural network analyses of ground surface settlement of tunnel in saturated soil. *SN Applied Sciences* 2:939, DOI: 10.1007/s42452-020-2742-z

Ghiasi V, Mozafari V (2018) Seismic response of buried pipes to microtunnelling method under earthquake loads. *Soil Dynamics and Earthquake Engineering* 113:193-201, DOI: 10.1016/j.soildyn.2018.05.020

González C, Sagaseta C (2001) Patterns of soil deformations around tunnels. Application to the extension of Madrid Metro. *Computers and Geotechnics* 28:445-468, DOI: 10.1016/S0266-352X(01)00007-6

Guha I, Randolph MF, White DJ (2016) Evaluation of elastic stiffness parameters for pipeline–soil interaction. *Journal of Geotechnical and Geoenvironmental Engineering* 142(6):04016009, DOI: 10.1061/(ASCE)GT.1943-5606.0001466

Kog YC, Kho C, Loh KK (2013) Tunnel design and modulus of subgrade reaction. *Journal of Performance of Constructed Facilities* 29(2): 04014065, DOI: 10.1061/(ASCE)CF.1943-5509.0000537

Jamil I, Ahmad I (2019) Bending moments in raft of a piled raft system using Winkler analysis. *Geomechanics and Engineering* 18(1):41-48, DOI: 10.12989/gae.2019.18.1.041

Luscher U (1966) Buckling of soil–surrounded tubes. *Journal of the Soil Mechanics and Foundations Division* ASCE 92(6):211-228, DOI: 10.1061/JSFEAQ.0000920

Matsubara K, Hoshiya M (2000) Soil spring constants of buried pipelines for seismic design. *Journal of Engineering Mechanics,* ASCE 126(1): 76-83, DOI: 10.1061/(asce)0733-9399(2000)126:1(76)

Okeagu B, Abdel-Sayed G (1984) Coefficients of soil reaction for buried flexible conduits. *International Journal of Geotechnical Engineering* 110:908-922, DOI: 10.1061/(asce)0733-9410(1984)110:7(908)

Prendergast LJ, Gavin K (2016) A comparison of initial stiffness formulations for small–strain soil–pile dynamic Winkler modelling. *Soil Dynamics and Earthquake Engineering* 81:27-41, DOI: 10.1016/j.soildyn.2015.11.006

Terzaghi K (1955) Evaluation of coefficients of subgrade reaction. *Geotechnique* 5(4):297-326, DOI: 10.1680/geot.1955.5.4.297

Timoshenko SP, Goodier JN (1951) Theory of elasticity, 2nd edn. McGraw–Hill, New York

Verruijt A (1997) A complex variable solution for a deforming circular tunnel in an elastic half-plane. *International Journal for Numerical and Analytical Methods in Geomechanics* 21(2):77-89, DOI: 10.1002/(SICI)1096-9853(199702)21:2<77::AID-NAG857>3.0.CO;2-M

Woo KS, Lee DW, Yang SH, Ahn JS (2018) Static behavior of a laterally loaded guardrail post in sloping ground by LS-DYNA. *Geomechanics and Engineering* 15(5):1101-1111, DOI: 10.12989/gae.2018.15.5.1101

Wood M (1975) The circular tunnel in elastic ground. *Geotechnique* 25(1):115-127, DOI: 10.1680/geot.1975.25.1.115

Yu Y, Shang YD, Sun HY (2014) A theoretical method to predict crack initiation in stabilizing piles. *KSCE Journal of Civil Engineering* 18(5):1332-1341, DOI: 10.1007/s12205-014-0063-8

Zhang D, Huang H, Phoon KK, Hu Q (2014) A modified solution of radial subgrade modulus for a circular tunnel in elastic ground. *Soils and Foundations* 54(2):225-232, DOI: 10.1016/j.sandf.2014.02.012

Zhang Y, Wang X, Wang X, Mang HA (2022) Virtual displacement based discontinuity layout optimization. *International Journal for Numerical Methods in Engineering* 123(22):5682-5694, DOI: 10.1002/nme.7084

Zhang Y, Zhuang X (2018) Cracking elements: A self-propagating strong discontinuity embedded approach for quasi-brittle fracture. *Finite Elements in Analysis and Design* 144:84-100, DOI: 10.1016/j.finel.2017.10.007

Zhang Y, Zhuang X (2019) Cracking elements method for dynamic

brittle fracture. *Theoretical and Applied* Fracture *Mechanics* 102:1-9, DOI: 10.1016/j.tafmec.2018.09.015

Zhang Y, Zhuang X, Lackner R (2018) Stability analysis of shotcrete supported crown of NATM tunnels with discontinuity layout optimization. *International Journal for Numerical and Analytical Methods in Geomechanics* 42(11):1199-1216, DOI: 10.1002/nag.2775

Appendix 1. Derivation

If a radial displacement, $u_r = u_0\sin(2\theta)$, is applied on the tunnel surface, the displacements in the x- and y- directions are

$$\begin{aligned} u_x &= u_r\cos(\theta) = u_0\sin(2\theta)\cos(\theta) \\ u_y &= u_r\sin(\theta) = u_0\sin(2\theta)\sin(\theta). \end{aligned} \tag{33}$$

The boundary in the region z can be written as:

$$2G\left(u_x + iu_y\right) = 2Gu_0\sin(2\theta)e^{i\theta}. \tag{34}$$

From the conformal transformation in Eqs. (4) and (5), the equations can be obtained:

$$\begin{aligned} e^{i\theta} &= i\frac{\alpha-\sigma}{1-\alpha\sigma} \\ \sin\theta &= \frac{z-\bar{z}+2ih}{2ir} = \frac{1+\alpha^2}{2\alpha} - \frac{\left(1-\alpha^2\right)^2}{2\alpha\left(1-\alpha\sigma\right)\left(1-\alpha\sigma^{-1}\right)} \\ \cos\theta &= \frac{x}{r} = \frac{z+\bar{z}}{2r} = \frac{i\left(1-\alpha^2\right)\left(\sigma^{-1}-\sigma\right)}{2\left(1-\alpha\sigma\right)\left(1-\alpha\sigma^{-1}\right)}, \end{aligned} \tag{35}$$

where $\sigma = e^{i\theta}$ represents a circle with a radius of 1.0 in the region ζ.

Substituting Eq. (35) into Eq. (34) gives

$$2G\left(u_x + iu_y\right) = \frac{Gu_0\left(1-\alpha^2\right)}{\alpha}\frac{\alpha-\sigma}{1-\alpha\sigma}\frac{\left(\alpha+\alpha^3\right)\sigma^{-2} - 4\alpha^2\sigma^{-1} + 4\alpha^2\sigma^1 - \left(\alpha+\alpha^3\right)\sigma^2}{\left(1-\alpha\sigma\right)^2\left(1-\alpha\sigma^{-1}\right)^2}. \tag{36}$$

According to Eqs. (15) and (36) can be written as

$$\sum_{k=-\infty}^{\infty} A_k\sigma^k = \frac{Gu_0\left(1-\alpha^2\right)}{\alpha}(\alpha-\sigma)\frac{\left(\alpha+\alpha^3\right)\sigma^{-2} - 4\alpha^2\sigma^{-1} + 4\alpha^2\sigma^1 - \left(\alpha+\alpha^3\right)\sigma^2}{\left(1-\alpha\sigma\right)^2\left(1-\alpha\sigma^{-1}\right)^2}. \tag{37}$$

Using the Taylor series expansion, the following equations can be obtained,

$$\frac{1}{\left(1-\alpha\sigma\right)\left(1-\alpha\sigma^{-1}\right)} = \frac{1}{1-\alpha^2}\left[\sum_{k=0}^{\infty}\alpha^{k+1}\sigma^{k+1} + \sum_{k=0}^{\infty}\alpha^k\sigma^{-k}\right], \tag{38}$$

$$\begin{aligned} \frac{\left(\alpha^2-1\right)^2}{\left(1-\alpha\sigma\right)^2\left(1-\alpha\sigma^{-1}\right)^2} &= \sum_{k=0}^{\infty}(k+1)(\alpha\sigma)^{k+2} + \sum_{k=0}^{\infty}(k+1)\alpha^k\sigma^{-k} + \\ &\sum_{k=0}^{\infty}\frac{2\alpha^{k+2}}{1-\alpha^2}\sigma^{k+2} + \sum_{k=0}^{\infty}\frac{2\alpha^{k+1}}{1-\alpha^2}\sigma^{-k+1} \end{aligned} \tag{39}$$

Substituting Eqs. (38) and (39) into Eq. (37) gives

$$\begin{aligned} \sum_{k=-\infty}^{\infty} A_k\sigma^k = \frac{Gu_0}{\alpha\left(1-\alpha^2\right)}&\left[\alpha^2+\alpha^4-\left(\alpha+5\alpha^3\right)\sigma+4\alpha^2\sigma^2+4\alpha^3\sigma^3-\left(5\alpha^2+\alpha^4\right)\sigma^4+\left(\alpha+\alpha^3\right)\sigma^5\right] \\ &\left[\sum_{k=0}^{\infty}(k+1)\alpha^{k+2}\sigma^k + \sum_{k=0}^{\infty}(k+1)\alpha^k\sigma^{-k-2} + \sum_{k=0}^{\infty}\frac{2}{1-\alpha^2}\alpha^{k+2}\sigma^k + \sum_{k=0}^{\infty}\frac{2}{1-\alpha^2}\alpha^{k+1}\sigma^{-k-1}\right]. \end{aligned} \tag{40}$$

The coefficients of all powers of σ on the left and right sides of Eq. (40) are equal, by which Eq. (25) can be obtained.